Inorg. Chem. **2005**, *44*, 7449–7458

Spectroscopy and Coordination Chemistry of a New Bisnaphthalene–Bisphenanthroline Ligand Displaying a Sensing Ability for Metal Cations

João Pina and J. Seixas de Melo*

Departamento de Química, Universidade de Coimbra, 3004-535 Coimbra, Portugal

Fernando Pina,* Carlos Lodeiro, J. C. Lima, and A. Jorge Parola

REQUIMTE/CQFB, Departamento de Química, Faculdade de Ciências e Tecnologia, Universidade Nova de Lisboa, 2829-516 Monte de Caparica, Portugal

Conxa Soriano

Departament de Química Orgánica, ICMOL, Facultat Farmacia,Universitat de València, 46100 Burjassot, Spain

M. Paz Clares, M. Teresa Albelda, Ricardo Aucejo, and Enrique García-España*

Departament de Química Inorgànica, ICMOL, Facultat de Química,Universitat de València, 46100 Burjassot, Spain

Received May 10, 2005

A new fluorescent macrocyclic structure (**L1**) bearing two naphthalene units at both ends of a cyclic polyaminic chain containing two phenanthroline units was investigated with potentiometric and fluorescence (steady-state and time-resolved) techniques. The fluorescence emission spectra show the simultaneous presence of three bands: a short wavelength emission band (naphthalene monomer), a middle emission band (phenanthroline emission), and a long-wavelength band. All three bands were found to be dependent on the protonation state of the macrocyclic unit (including the polyaminic and phenanthroline structures). The existence of the long-wavelength emission band is discussed and is shown to imply that a bending movement involving the two phenanthroline units leads to excimer formation. This is determined by comparison with the excimer emission formed by intermolecular association of 1,10-phenanthroline. With ligand **L1**, excimer formation occurs only at pH values above 4. At very acidic pH values, the protonation of the polyamine bridges is extensive leading to a rigidity of the system that precludes the bending movement. The interaction with metal cations Zn(II) and Cu(II) was also investigated. Excimer formation is, in these situations, increased with Zn(II) and decreased with Cu(II). The long-emission band is shown to present a different wavelength maximum, depending on the metal, which can be considered as a characteristic to validate the use of ligand **L1** as a sensor for a given metal.

Introduction

Multichromophoric structures have received an increased interest in the recent years. In part, this interest arose from their potential applications in fields of very high impact, such as molecular recognition, fluorescence sensors, molecular devices, etc.[1−4] In the particular case of fluorescence sensors,

* To whom correspondence should be addressed. E-mail: sseixas@ci.uc.pt. Phone: 351 239854463. Fax: 351 239 827703 (J.S.d.M.). E-mail: fjp@dq.fct.unl.pt (F.P.). E-mail: enrique.garcia-es@uv.es. Phone: 963544879. Fax: 963544879 (E.G.-E.).

(1) deSilva, A. P.; Gunaratne, H. Q. N.; Gunnlaugsson, T.; Huxley, A. J. M.; McCoy, C. P.; Rademacher, J. T.; Rice, T. E. *Chem. Rev.* **1997**, *97*, 1515−1566.
(2) Pina, F.; Melo, M. J.; Bernardo, M. A.; Luis, S. V.; Garcia-España, E. *J. Photochem. Photobiol. A* **1999**, *126*, 65−69.

10.1021/ic050733q CCC: $30.25
Published on Web 09/16/2005

Chart 1

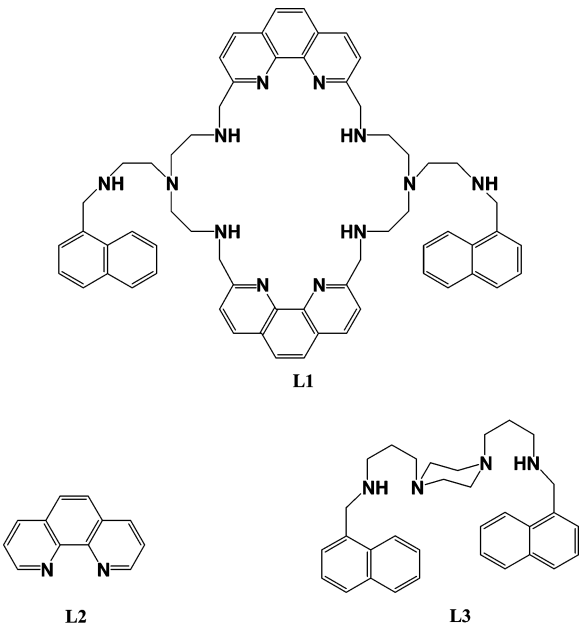

the design of ligands (as therapeutic agents for the treatment of metal intoxication), antibiotics (that owe their antibiotic action to specific metal coordination), complexes (to act as imaging agents in the body), and functional groups for chelating ion-exchange materials has deserved a particular attention from the photochemistry sciences.

Polyamine systems bearing fluorescent units have been extensively studied by our groups for the last 10 years with regard to their potential activity as pH sensors, molecular devices, metal sensors, etc. Recently, the effort in the development of new molecules able to perform movements and to signal transition metals was put in three new compounds bearing *m*-phenylene, *p*-phenylene, or azapyridinophane spacers that were symmetrically appended to aminoethyl naphthyl moieties.[5,6] In the present work, we are extending these studies to a new compound in which the spacer incorporates aminic units and with 1,10-phenanthroline (Chart 1). The use of 1,10-phenanthroline can be considered an improvement from the point of view of sensing cations.[5,6] It is well-known that 1,10-phenanthroline forms stable complexes with different kinds of metals[7] and is used as a redox indicator for Fe(III).[8] From this point of view, a molecule that incorporates this ligand will potentially display sensing ability toward metal cations.

We have pursued one additional question in past years regarding the movements of molecules induced by light. In previous works, with aromatic fluorescent (naphthalenes, pyrenes, and anthracenes) units, we have shown that the excitation of single units can give rise to new species resulting from excimer[6,9−12] or exciplex[13,14] formation and energy transfer.[2,15] With the present system, we will show the formation of a new excimer involving two phenanthroline units. To our best knowledge, it is the first time that intramolecular (in concentrated and pH-dependent 1,10-phenanthroline solutions) excimer formation with phenanthroline is reported.

The present work reports the fluorescence properties of a new ligand possessing two naphthalene and two phenanthroline chromophores (**L1** in Chart 1). For comparison purposes, compounds **L2** (1,10-phenanthroline) and **L3** (bischromophoric naphthalene compound with a rigid piperazine unit as spacer) were also considered, and in the former case, their properties were investigated parallel to **L1**. Compound **L3** can be used as a model compound for the study of molecular movements in similar naphthalene-type molecules.[10,11] This relies on its structural rigidity which avoids the contact proximity between the two naphthalene moieties, thus excluding intramolecular excimer formation.[10,11] In regard to the metal sensing ability, compound **L2** constitutes the fundamental moiety of ligand **L1** for metal coordination. Its fluorescence properties are also pH dependent and were therefore also characterized by steady-state and time-resolved techniques.

Experimental Section

Synthesis. 1,10-Phenanthroline-2,9-dicarboxaldehyde. 1,10-Phenanthroline-2,9-dicarboxaldehyde was prepared as described in ref 16. N^1-(2-Amino-ethyl)-N^1-{2-[(naphthalen-1-ylmethyl)-amino]-ethyl}-ethane-1,2-diamine was synthesized as described elsewhere.

Naphthalen-1-ylmethyl-[2-(23-{2-[(naphthalen-1-ylmethyl)-amino]-ethyl}-3,6,9,22,25,28-hexaaza-tricyclo[26.8.4.4]triaconta-1(38),14(39),15,17,33,36-hexaen-6-yl)-ethyl]-amine Nonaclorhydrate (L1). The synthesis of compound **L1** was carried out by a 2:2 dipodal condensation in ethanol of the tripodal polyamine tren monofunctionalized with a methyl naphthalene group and the corresponding 1,10-phenanthroline-2,9-dicarboxaldehyde. N^1-(2-Amino-ethyl)-N^1-{2-[(naphthalen-1-ylmethyl)-amino]-ethyl}-ethane-1,2-diamine (1.01 g, 3.53 mmol) and 1,10-phenanthroline-2,9-

(3) Badjic, J. D.; Balzani, V.; Credi, A.; Lowe, J. N.; Silvi, S.; Stoddart, J. F. *Chem.—Eur. J.* **2004**, *10*, 1926−1935.
(4) Badjic, J. D.; Balzani, V.; Credi, A.; Silvi, S.; Stoddart, J. F. *Science* **2004**, *303*, 1845−1849.
(5) Sabatini, A.; Vaca, A.; Gans, A. *Coord. Chem. Rev.* **1992**, *120*, 389−405.
(6) Seixas de Melo, J.; Pina, J.; Pina, F.; Lodeiro, C.; Parola, A. J.; Lima, J. C.; Albelda, M. T.; Clares, M. P.; Garcia-España, E. *J. Phys. Chem. B* **2003**, *107*, 11307−11318.
(7) Hancock, R. D.; Martell, A. E. *Chem. Rev.* **1989**, *89*, 1875−1914.
(8) Skoog, D. A.; West, D. M.; Holler, F. J.; Crouch, S. R. *Analytical Chemistry. An Introduction*, 7th ed.; Harcourt: Orlando, FL, 2000.
(9) Albelda, M. T.; Garcia-España, E.; Gil, L.; Lima, J. C.; Lodeiro, C.; Seixas de Melo, J.; Melo, M. J.; Parola, A. J.; Pina, F.; Soriano, C. *J. Phys. Chem. A* **2003**, *107*, 6573−6578.
(10) Seixas de Melo, J.; Albelda, M. T.; Diaz, P.; Garcia-España, E.; Lodeiro, C.; Alves, S.; Lima, J. C.; Pina, F.; Soriano, C. *J. Chem. Soc., Perkin Trans. 2* **2002**, 991−998.
(11) Bernardo, M. A.; Alves, S.; Pina, F.; Seixas de Melo, J.; Albelda, M. T.; Garcia-España, E.; Llinares, J. M.; Soriano, C.; Luis, S. V. *Supramol. Chem.* **2001**, *13*, 435−445.
(12) Albelda, M. T.; Bernardo, M. A.; Diaz, P.; Garcia-España, E.; Seixas de Melo, J.; Pina, F.; Soriano, C.; Santiago, V. L. E. *Chem. Commun.* **2001**, 1520−1521.
(13) Bencini, A.; Berni, E.; Bianchi, A.; Fornasari, P.; Giorgi, C.; Lima, J. C.; Lodeiro, C.; Melo, M. J.; Seixas de Melo, J.; Parola, A. J.; Pina, F.; Pina, J.; Valtancoli, B. *Dalton Trans.* **2004**, 2180−2187.
(14) Bencini, A.; Bianchi, A.; Lodeiro, C.; Masotti, A.; Parola, A. J.; Pina, F.; Seixas de Melo, J.; Valtancoli, B. *Chem. Commun.* **2000**, 1639−1640.
(15) Albelda, M. T.; Diaz, P.; Garcia-España, E.; Lima, J. C.; Lodeiro, C.; Seixas de Melo, J.; Parola, A. J.; Pina, F.; Soriano, C. *Chem. Phys. Lett.* **2002**, *353*, 63−68.
(16) Chandler, C. J.; Deady, L. W.; Reiss, J. A. *J. Heterocycl. Chem.* **1981**, *18*, 599−601.

dicarboxaldehyde (0.49 g, 3.53 mmol) were stirred for 3 h in 75 mL of EtOH. Sodium borohydride (1.07 g, 0.028 mmol) was added to the above solution, and the mixture was stirred for 1 h. The solvent was removed under reduced pressure. The resulting residue was treated with water, and the difunctionalized amine was repeatedly extracted with dichloromethane (3 × 30 mL). The organic phase was dried with anhydrous sodium sulfate, and the solvent was evaporated to yield the free amine, which was dissolved in ethanol and precipitated as its hydrochloride salt. Yield: 30%. mp: 215−217 °C. NMR (solvent D_2O): δ_H 2.96 (t, $J = 5$ Hz, 2H), 3.05 (t, $J = 6$ Hz, 4H), 3.24 (t, $J = 6$ Hz, 2H), 3.39 (t, $J = 6$ Hz, 4H), 4.33 (s, 2H), 4.50 (s, 4H), 6.87 (t, $J = 8$ Hz, 1H), 7.12−7.15 (m, 2H), 7.30 (d, $J = 7$ Hz, 2H), 7.39−7.48 (m, 2H), 7.68 (d, $J = 8$ Hz, 2H), 7.83 (s, 2H), 8.41 (d, $J = 8$ Hz, 2H). NMR: δ_C 46.5, 48.7, 52.5, 53.3, 55.7, 122.1, 124.3, 125.8, 125.9, 126.4, 126.8, 128.1, 128.6, 132.5, 133.3, 133.6, 135.7, 144.5, 160.1. Anal. Calcd for $C_{62}H_{77}N_{12}Cl_9$: C, 56.87; H, 5.93; N, 12.84. Found: C, 56.2; H, 6.1; N, 12.1.

Potentiometric Measurements. The potentiometric titrations were carried out in the mixed solvent H_2O/C_2H_5OH (70:30 v/v) at 298.1 ± 0.1 K using NaCl (0.15 mol dm^{-3}) as supporting electrolyte. The experimental procedure (buret, potentiometer, cell, stirrer, microcomputer, etc.) has been fully described elsewhere.[17] The acquisition of the emf data was performed with the computer program PASAT.[18] The reference electrode was an Ag/AgCl electrode in saturated KCl solution. The glass electrode was calibrated as an hydrogen-ion concentration probe by titration of previously standardized amounts of HCl with CO_2-free NaOH solutions and by determining the equivalent point by the Gran's method,[19] which gives the standard potential, $E°'$, and the ionic product of water in this medium ($pK_w = 14.16(1)$).[20]

The computer program HYPERQUAD was used to calculate the protonation and stability constants.[5] The pH range investigated (pH $= -\log[H^+]$) was 2.0−11.0. The different titration curves for each ligand were treated as separated curves without significant variations in the values of the stability constants. Finally, the sets of data were merged together and treated simultaneously to give the final stability constants.

Spectrophotometric and Spectrofluorimetric Measurements. The solvents used were of spectroscopic or equivalent grade. Water was twice distilled and passed through a Millipore apparatus. All aqueous solutions were prepared in 0.15 mol dm^{-3} NaCl. The measured pH values were obtained with a Crison micropH 2000 and adjustments of the hydrogen ion concentration of the solutions were made with diluted HCl and NaOH solutions.

Absorption and fluorescence spectra were recorded on Shimadzu UV-2100 and Jovin-Yvon Spex Fluorog 3−2.2. spectrometers, respectively. Fluorescence spectra were corrected for the wavelength response of the system. The fluorescence quantum yield of compound **L3** was determined using naphthalene ($\phi_F = 0.21$ in ethanol[21]) as standard. The fluorescence quantum yields for compounds **L1** and **L2** were measured in aqueous solution for different values of pH, using the previously obtained value for the **L3** compound [$\phi_F(H_2O, pH\ 2.5) = 0.43$][6] as reference.

L3 was used as standard to obtain the fluorescence quantum efficiency for the excimer (ϕ_F^E) occurring with the **L1** and **L2** compounds, and the total fluorescence quantum yield, ϕ_F^T, was obtained using of the equation[6]

$$\phi_F^{\,E} = \frac{\phi_E^{\,Ap}}{1 - \dfrac{\phi_M^{\,Ap}}{\phi_F^{\,M}}}$$

where the apparent fluorescence yields, ϕ_E^{Ap} and ϕ_M^{Ap}, result from the integrated areas under the excimer and monomer bands respectively, with $\phi_F^T = \phi_{Exc}^{Ap} + \phi_M^{Ap}$, and ϕ_F^M is the fluorescence quantum yield of the reference (**L3**) compound considered as the monomer. The I_E/I_M ratio results from the decomposed area under the monomer and excimer bands. The general procedure to obtain those values involves matching the emission spectra of **L1** in water with the monomer band of compounds **L2** and **L3**, after which the match of the relative intensities and vibronic band progression is almost identical for the **L2**, **L3**, and **L1** compounds. The resulting differential spectrum is the excimer band.

Fluorescence decays were measured using a home-built TCSPC apparatus with an D_2/N_2 filled IBH 5000 coaxial flashlamp as excitation source or alternatively with a Horiba-JI-IBH nanoLED (281 and 339 nm), Jobin-Yvon excitation and emission monochromators, Philips XP2020Q photomultiplier, and Canberra instruments TAC and MCA.[22] The fluorescence decays were analyzed using the method of modulating functions implemented by Striker.[23]

1,10-Phenanthroline was purchased from Merck and used upon recrystalization. To obtain reproducible results, ultrapure water from Merck was used, and the phenanthroline solution was kept overnight at pH 10 and filtered before the titrations. The fluorescence emission spectra of the concentrated solutions were carried out with the fluorimeter in the front face geometry, while those of the diluted solutions were performed at a right angle geometry. The fluorescence emission titration curves were obtained upon excitation at the isosbestic point at 265 nm. The emission from the basic form was collected at 360 nm and the acid at 420 nm. The contribution of the fluorescence emission from the basic species at 420 nm was subtracted to obtain the net fluorescence emission from the acidic species and vice versa, following the procedure previously reported in the literature.[6]

Results and Discussion

Potentiometric Studies. Table 1 lists the protonation constants of **L1**, and Table 2 shows the stability constants for the systems Cu(II)−**L1** and Zn(II)−**L1** determined in the mixed solvent H_2O/EtOH (70:30 v/v).

Although the compound was isolated as its nonachlorhydrate salt, it was just possible to measure seven protonation constants in the pH range of 2−11 explored by potentiometry. The first six protonation constants are relatively large with values ranging from 10.71 to 5.59 while the constant for the seventh protonation step is much lower. The first six constants that can be organized in three groups of two constants should correspond to the protonation of the four secondary nitrogen atoms in the macrocyclic core at each side of the phenanthroline fragments and to the two second-

(17) Garcia- España, E.; Ballester, M. J.; Lloret, F.; Moratal, J. M.; Faus, J.; Bianchi, A. *J. Chem. Soc., Dalton Trans.* **1998**, 101.
(18) Fontanelli, M.; Micheloni, M. *Proceedings of the I Spanish-Italian Congress on Thermodynamics of Metal Complexes*; Diputación de Castellón: Castellón, Spain, 1990.
(19) Gran, G. *Analyst* **1952**, *77*, 661−671.
(20) Avdeef, A.; Box, K. J.; Comer, J. E. A.; Gilges, M.; Hadley, M.; Hibbert, C.; Patterson, W.; Tam, K. Y. *J. Pharm. Biomed. Anal.* **1999**, *20*, 631−641.
(21) Murov, S.; Charmichael, I.; Hug, G. L. *Handbook of Photochemistry*; M. Dekker Inc.: New York, 1993.
(22) Seixas de Melo, J.; Fernandes, P. F. *J. Mol. Struct.* **2001**, *565−566*, 69.
(23) Stricker, G.; Subramaniam, V.; Seidel, C. A. M.; Volkmer, A. *J. Phys. Chem. B* **1999**, *103*, 8612−8617.

Table 1. Stepwise Protonation Constants for **L1** Determined in NaCl 0.15 mol dm^{-3} ($EtOH/H_2O$, 3:7) at 298.0 ± 0.1 K

reaction[a]	**L1**[b]	**L**[c]
$L + H \leftrightarrows HL$	10.71(5)	9.46
$HL + H \leftrightarrows H_2L$	9.82(4)	8.46
$H_2L + H \leftrightarrows H_3L$	8.67(6)	7.65
$H_3L + H \leftrightarrows H_4L$	8.00(6)	7.25
$H_4L + H \leftrightarrows H_5L$	6.69(7)	6.50
$H_5L + H \leftrightarrows H_6L$	5.59(8)	6.29
$H_6L + H \leftrightarrows H_7L$	3.65(9)	
$\log \beta$	53.13	

[a] Charges omitted for clarity. [b] Numbers in parentheses are standard deviations in the last significant figure. [c] Taken from ref 31 (see ligand **L** in reference ref 31).

Table 2. Stability Constants for the Interaction of **L1** with Cu^{2+} and Zn^{2+} Determined in NaCl 0.15 mol dm^{-3} ($EtOH/H_2O$, 3:7) at 298.0 ± 0.1 K

reaction[a]	Cu^{2+} [b]	Zn^{2+}
$M + L \leftrightarrows ML$	14.50(8)	10.6(1)
$M+ L + H \leftrightarrows MHL$	25.33(9)	22.04(8)
$M + L + 2H \leftrightarrows MH_2L$	35.14(8)	32.27(6)
$M + L + 3H \leftrightarrows MH_3L$	42.68(7)	39.48(5)
$M + L + 4H \leftrightarrows MH_4L$	48.14(4)	45.58(3)
$2M + L \leftrightarrows M_2L$	25.10(9)	17.06(9)
$2M + L + H \leftrightarrows M_2HL$	35.02(1)	−
$2M + L + 2H \leftrightarrows M_2H_2L$	43.67(6)	−
$2M + L + OH \leftrightarrows M_2(OH)L$	14.29(1)	6.87(6)
$ML + H \leftrightarrows MHL$	10.83(4)	11.41(5)
$MHL + H \leftrightarrows MH_2L$	9.81(2)	10.24(3)
$MH_2L + H \leftrightarrows MH_3L$	7.54(2)	7.21(2)
$MH_3L + H \leftrightarrows MH_4L$	5.46(3)	6.10(2)
$M_2L + H \leftrightarrows M_2HL$	9.93(2)	−
$M_2HL + H \leftrightarrows M_2H_2L$	8.64(3)	−
$ML + M \leftrightarrows M_2L$	10.60(5)	6.44(5)

[a] Charges omitted for clarity. [b] Numbers in parentheses are standard deviations in the last significant figure.

ary amino groups in the pendant arms of the bibrachial lariat ether. The values of these stability constants are similar although slightly larger than those previously calculated in aqueous solution for the related macrocycles containing *m*-xylene, *p*-xylene, or 2,5-dimethylpyridine spacers between the tripodal fragments, which can be attributed to the lower ionization product of water in the mixed solvent ($pK_w = -14.16$ in ethanol/water 3:7 v/v vs -13.73 in pure water under the same experimental conditions).[6,24]

The seventh protonation should most likely occur on one of the phenanthroline subunits as it has been proved by the changes in the electronic absorption and emission spectra of **L1** that occur at low pH (vide infra Figures 1 and 2 and related text).

Cu^{2+} and Zn^{2+} Interaction. The logarithms of the stability constants for the formation of the Cu^{2+} and Zn^{2+} complexes of **L1** collected in Table 2 show that the Cu^{2+} complexes are by far more stable than the Zn^{2+} ones. For instance, there are almost 4 orders of magnitude difference between the stability constants of $Cu\mathbf{L1}^{2+}$ and $Zn\mathbf{L1}^{2+}$ (Table 2). The formation constants for the Cu^{2+} complexes are low in comparison with those obtained for tetraamines of different kinds.[25] On the other hand, the stepwise protonation constants of the complexes are very high supporting that these processes occur on noncoordinated nitrogen atoms. Moreover, it is interesting to remark that the values of the stability constants for the Cu^{2+} complexes are lower than those obtained in pure water for the related macrocycle containing pyridine spacers between the polyamine bridges instead of phenanthroline ones.[24] These data suggest that, in the mononuclear complexes, Cu^{2+} binds at the phenanthroline units with little participation of the other metal atoms.

Both metal ions also form dinuclear metal complexes. While for copper, $[Cu_2H_rL]^{(4+r)+}$ species with r between 2 and -1 have been found, in the case of Zn^{2+}, just the $[Zn_2L]^{4+}$ neutral and $[Zn_2L(OH)]^{3+}$ monohydroxylated species were detected in solution. Again, the constants obtained for the binuclear Cu^{2+} species are not very large and suggest the presence of noncoordinated amine nitrogens. In the distribution diagrams (Supporting Information), it can be seen that the nuclearity of the predominant species in solution is highly dependent on the Cu^{2+}/**L1** mole ratio.

Absorption and Fluorescence Properties. The absorption spectra of compound **L1** results from the overlap of the individual **L2** (phenanthroline) and **L3** spectra; albeit the lack of coincidence between this sum (**L2** + **L3**) and the **L1** spectra suggests the existence of some ground-state interaction between the different moieties (see Supporting Information for further details).

The fluorescence emission spectrum of **L1**, obtained at different pH values, is shown in Figure 1A. The spectrum consists of three emissive bands (Figure 1B): (i) one of higher energy (emission maximum at ≈ 323 nm) coincident with the emission of compound **L3** (naphthalene origin), (ii) an intermediate energy emission band (emission maximum at ≈ 366 nm) which can be assigned to the phenanthroline moiety, **L2**, and (iii) a broad red-shifted unstructured emission band, centered at ≈ 460 nm, whose intensity is dependent on pH, reaching a maximum around pH 5. The fluorescence spectrum of this last emission band can be obtained upon subtraction of the emissions from **L2** and **L3** as shown in Figure 1B.

Figure 2 shows the pH dependence of the mole fraction distribution for the different species of compound **L1**. This distribution pattern is relevant not only to the attribution of the different species but also to the identification of the nature of the long-wavelength emitting species. The overall data reveals that the long-wavelength emission band only occurs for pH values above 4. Moreover, for pH < 4, the emission intensity is, at 366 nm (phenanthroline emission), higher than that observed at 323 nm (naphthalene emission).

As will be shown below, the fluorescence emission spectrum of 1,10-phenanthroline (**L2**) decreases in intensity and is red shifted upon protonation. On this basis, it can be concluded that the phenanthroline moiety is not protonated up to pH 2 because its emission is still high at acidic pH values, which can be explained by the electrostatic repulsion of the protons linked to the polyamine chain. However, at higher pH values, a significant quenching of this emission occurs.

(24) Kelly, R. N.; Schulman, S. G. In *Molecular Luminescence Spectroscopy. Methods and Applications: Part 2*; Schulman, S. G., Ed.; Willey: New York, 1985.
(25) Seixas de Melo, J.; Costa, T.; Miguel, M. d. G.; Lindman, B.; Schillén, K. *J. Phys. Chem. B* **2003**, *107*, 12605−12621.

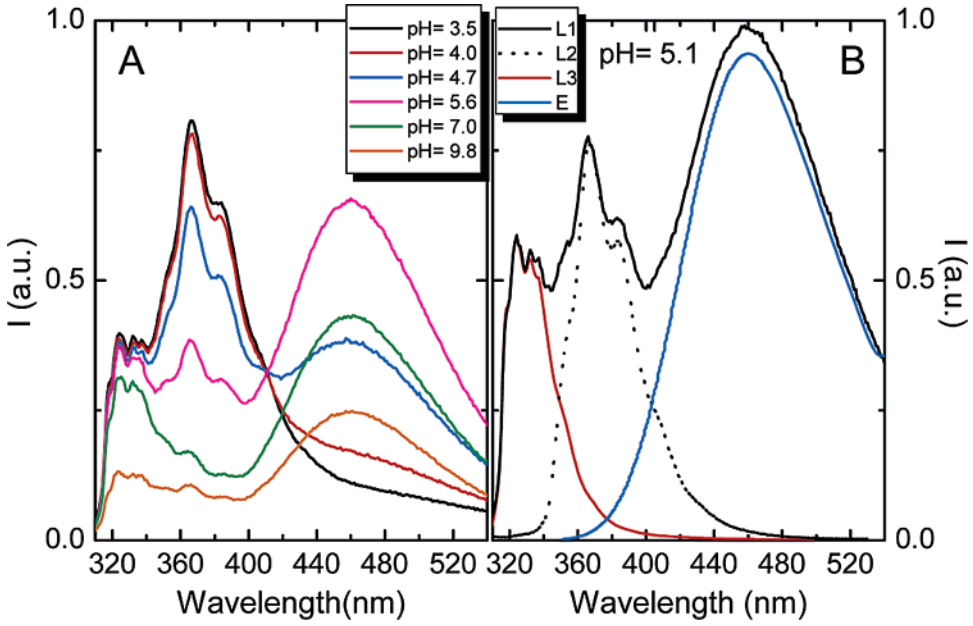

Figure 1. (A) Fluorescence emission spectra of **L1** at different pH values, $\lambda_{exc} = 275$ nm. (B) Decomposition of the fluorescence emission spectrum of compound **L1** at pH 5.1, in their three components **L1**, **L2**, and adduct.

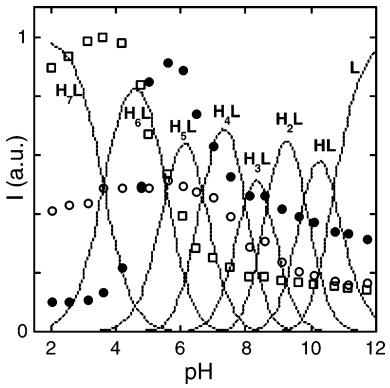

Figure 2. Steady-state fluorescence emission titration curves of **L1** ($\lambda_{exc} = 275$ nm) for an aqueous solution containing 1.07×10^{-5} M of **L1** and 0.15 M NaCl. Emission obtained with $\lambda_{exc} = 275$ nm and followed at $\lambda_{em} = 323$ (○), 366 (□), and 460 nm (●) at $T = 20$ °C. The dashed lines represent the molar fractions of the species, obtained from potentiometric titrations.

The fluorescence of the naphthalene moiety follows the behavior of this fluorophore when linked to a polyamine chain.[12,26] A progressive increase in the pH leads to the formation of a new deprotonated LH_n species with a concomitant gradual decrease in the total emission fluorescence. This is compatible with a long-range electron-transfer quenching from the deprotonated amines of the polyamine chains to both aromatic units.[26] On the other hand, such a quenching is not expected from the phenanthroline where the lone pairs are less available.

As can be seen in Figure 2, it is clear that the increase in intensity of the 460 nm band above pH 4 is associated with the decrease of the 366 nm band (phenanthroline emission), while the naphthalene moiety emission intensity does not change appreciably up to pH 6.

Origin of the 460 nm Band. One important issue of this study is to address the origin of the 460 nm band. Because of the low concentrations used in our experiments, such a band must be the result of an intramolecular associative phenomenon. In theory, this can have four possible origins: (1) excimer formation between the two naphthalene units, (2) formation of a charge transfer (CT) excited-state involving the amines and naphthalene groups, (3) exciplex formation between one phenanthroline and one naphthalene, and (4) excimer formation between the two phenanthroline units. The first hypothesis can be discarded because the emission maximum for the intramolecular naphthalene excimer has been found to be ∼390 nm in similar systems.[10,12] The possibility of a charge-transfer excited state (as seen for example in dendrimers functionalized at the periphery with naphthylsulfonamide units[27]) formed between the excited naphthalene and the amine units being responsible for this new emission can also be discarded since this structureless band does not occur with **L3** or with compounds containing a single naphthalene unit.[12,26] In fact, the formation of an excimer or an exciplex involving naphthalene can be easily discarded (which automatically excludes 3) because there is no observable quenching of the naphthalene moiety emission upon the formation of the species responsible for the emission at 460 nm.

At very acidic pH values, the fluorescence excitation spectra of **L1** collected at 324 and 366 nm only reveal the characteristic absorption spectra of the naphthalene (Np) and phenanthroline (**L2**) chromophores, respectively, (see Figure 3). For pH > 4, the excitation spectra collected at 460 nm, leads to the appearance of a new band, lying between those of the Np and **L2** chromophores (Figure 3B). Note that, at pH 1.4, the 460 nm emission is absent, whereas at pH 4.8, this band can be clearly observed (Figures 1 and 2). It can also be observed from Figure 3B that the band resulting from

(26) Pina, F.; Lima, J. C.; Lodeiro, C.; Seixas de Melo, J.; Diaz, P.; Albelda, M. T.; Garcia-España, E. *J. Phys. Chem. A* **2002**, *106*, 8207−8212.
(27) Pina, F.; Maestri, M.; Balzani, V.; Vogtle, F. *ChemPhysChem* **2004**, *5*, 473−480.

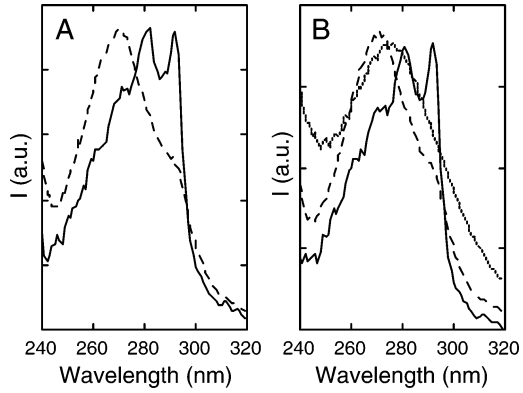

Figure 3. Normalized fluorescence excitation spectra of **L1** collected at 324 (full line), 366 (dash line) and 460 nm (dots) at two different pH values: (A) pH 1.4 and (B) pH 4.8.

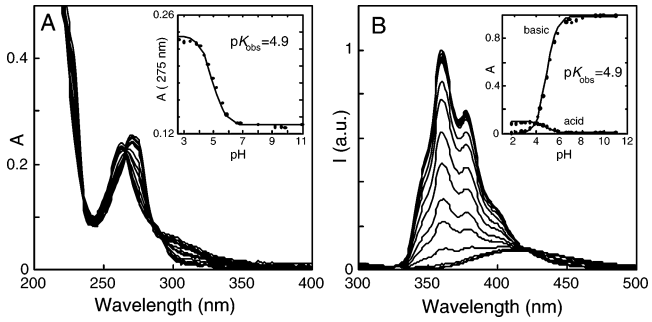

Figure 4. Absorption (A) and fluorescence emission (B) spectra of 1,10-phenanthroline as a function of pH. The fluorescence emission from the acidic (420 nm) and basic (360 nm) forms was separated according to the well-established procedure reported in the literature[28] (see inset Figure 1B). Excitation wavelength at the isosbestic point (265 nm).

collecting at 460 nm has a different maximum than the band collected at the Np and 1,10-phenanthroline emission regions. Moreover, this band overlaps with the absorption band of the **L1** ligand which gives positive evidence for the fact that this new band arises from the ground-state interaction of chromophores within the same **L1** molecule. In addition, Figure 2 gives evidence that this interaction should involve the two phenanthroline units, whose interaction leads to an emissive adduct. If this intramolecular interaction occurs, the question *what can be expected for a ground-state intermolecular analogue in 1,10-phenanthroline* needs to be answered. According to our best knowledge, there is no literature reporting the fluorescence emission from 1,10-phenanthroline in concentrated solutions, and thus, the observation of the intermolecular interaction could not have been made previously.

In Figure 4, the absorption and emission spectra of 1,10 phenanthroline, **L2**, at a concentration of 2.8×10^{-5} M are shown. An inspection of this figure shows that the protonation of this compound takes place at $pK_a = 4.9$ in agreement with the values previously reported in the literature.[28] The absorption spectra of the acidic form is red shifted, as usually found for heterocyclic compounds containing amines.[24] The pK_a of the ground and excited states are coincident, in accordance to the results previously reported by Schulman.[28]

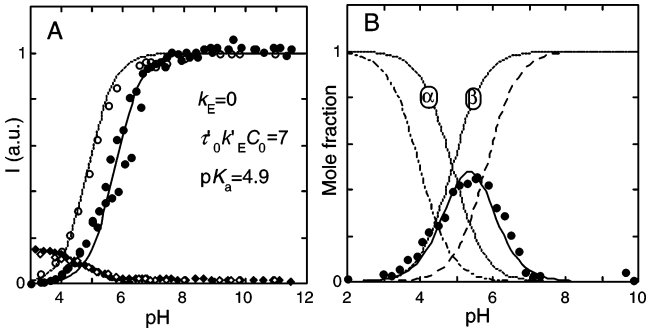

Figure 5. (A) Fluorescence emission titration curves of 1,10-phenanthroline: 3.5×10^{-6} M, $\lambda_{em} = 360$ nm, basic form emission (○), $\lambda_{em} = 420$ nm, acidic form emission (◇) and 6.9×10^{-3} M, front face measurements, basic form emission, $\lambda_{em} = 360$ nm, (●), $\lambda_{em} = 420$ nm, acidic form emission (◆). In all cases, the excitation was at $\lambda_{exc} = 265$ nm. Separation of the contributions from the acidic species in the basic emission and vice versa were carried out. (B) α and β represent the mole fraction distribution of the acidic and basic forms, respectively, of 1,10-phenanthroline; the traced line refers the difference between the fluorescence emission titration curves of the diluted and concentrated solutions of 1,10-phenanthroline. This last curve is coincident with that generated from eq 1 with $pK_a = 4.9$ and $\tau_0 k'_E C_0 = 7$. The traced-pointed line shows eq 2 for $pK_a = 4.9$ and $\tau_0 k_E C_0 = 7$. The fluorescence emission intensity at 510 nm for a 6.9×10^{-3} M concentration is shown by ●. The fitting of these experimental points can be done using eq 3.

Despite that, excited-state protonation of the nitrogens is expected because of the increased excited-state basicity of heterocycles containing amines.[24] This coincidence has been explained by the fact that the radiative and nonradiative decays of the excited species are faster than the proton transfer, preventing excited-state acid−base equilibrium from being reached.

In this work, we have extended the study of the 1,10-phenanthroline (**L2**) fluorescence emission to concentrated solutions with the aim of checking possible intermolecular excimer formation. This possibility was triggered by some descriptions of intramolecular excimer formation in compounds bearing two phenanthroline units,[29,30] as well as by our above-reported observation of the same phenomenon in the case of compound **L1**.

The fluorescence emission spectra of the concentrated 1,10-phenanthroline as a function of pH, is similar to that found for diluted solutions; however, they exhibit an additional weak emission band centered at ca. 510 nm, as well as a pH shift of the fluorescence emission titration curves of the basic species. The adduct emission band can be obtained upon subtraction of the emission of the concentrated solution from the one of the diluted solution (see Supporting Information).

Moreover, it can also be seen that the fluorescence emission titration curve of the basic species (black circles, Figure 5A) is shifted to higher pH values in comparison with the fluorescence emission titration curve of the diluted solutions (open circles in Figure 5A). On the other hand,

(28) Schulman, S. G.; Tidwell, P. T.; Cetorelli, J. J.; Winefordner, J. D. *J. Am. Chem. Soc.* **1971**, *93*, 3179−3183.

(29) Chouai, L.; Wu, F. Y.; Jang, Y. C.; Thummel, R. P. *Eur. J. Inorg. Chem.* **2003**, 2774−2782.

(30) Hayashi, K.; Akutsu, H.; Ozaki, H.; Sawai, H. *Chem. Commun.* **2004**, 1386-1387.

(31) Clares, M. P.; Aguilar, J.; Aucejo, R.; Lodeiro, C.; Albelda, M. T.; Pina, F.; Lima, J. C.; Parola, A. J.; Pina, J.; Seixas de Melo, J.; Soriano, C.; García-España, E. *Inorg. Chem.* **2004**, *43*, 6114−6122.

the fluorescence emission titration curves of the acidic species are, within experimental error (black and open squares in Figure 5A), coincident with concentrated or diluted solutions. A decrease in the 1,10-phenanthroline concentration, for example, to one-half (not shown) results in a shift of the titration curve to lower pH values.

In principle, the difference between the diluted and concentrated titration curves of 1,10-phenanthroline should represent the pH domain of the adduct which is formed in concentrated solutions (see the solid line in Figure 5B). This species is not observed at high pH values when there is no ground, excited acidic, or both form of phenanthroline, as well as low pH values when no ground, excited basic, or both form of phenanthroline are available. One possible explanation for this behavior is the formation of an adduct (possibly an excimer), involving one excited acidic and one ground-state basic phenanthroline units. This assumption is in agreement with the representation of the weak fluorescence emission (at 510 nm) dependence on the pH, which leads to a bell-shape curve (see Figure 5B).

As shown in Supporting Information, the formation of the intermolecular adduct can be accounted for by eq 1, eq 2, or both

$$PH^{+}* + P \rightarrow E \quad k_E \tag{1}$$

$$P* + PH^{+} \rightarrow E \quad k'_E \tag{2}$$

where PH^+ and P are respectively the acidic and basic forms of 1,10-phenanthroline and k_E and k'_E are the rate constants for excimer (E) formation at the expenses of one excited $PH^{+}*$ and one nonexcited P species or vice-versa (P* and PH^+). The fluorescence emission of the acidic, basic, and adduct species are given respectively by eqs 3−5 (see Supporting Information)

$$h\upsilon_1{}^n = \frac{\alpha}{1 + \tau_0 C_0 k_E \beta} \tag{3}$$

$$h\upsilon_2{}^n = \frac{\beta}{1 + \tau'_0 C_0 k'_E \alpha} \tag{4}$$

$$h\upsilon_3 = \Phi_{fE} \frac{\beta}{\frac{1}{\tau'_0 k'_E C_0 \alpha} + 1} \tag{5}$$

where

$$\Phi_{fE} = \frac{k_{iE}}{K_{iE} + K_{cE}}$$

is the fluorescence emission quantum yield of the adduct.

Eqs 3 and 4 are simulated in Figure 5B for $\tau_0 C_0 k_E$ and $\tau_0 C_0 k'_E = 7$ (traced-pointed lines and traced lines, respectively). An inspection of Figure 5B immediately excludes eq 1 because it would predict a shift of the fluorescence emission titration curves of the acidic species to lower pH values. On the contrary, the experimental results point to a coincidence between these two curves (Figure 5A). In other words, k_E is zero. On this basis, the adduct should be formed between the excited basic form of 1,10-phenanthroline and its ground-state acidic species. Moreover, using the lifetime of the basic species (see below), the rate constant $k_E = 1.7 \times 10^{11}\ s^{-1}\ M^{-1}$ can be calculated. As the term $\tau'_0 k'_E C_0$ was calculated above, the shape of the curve can be immediately determined, and the results are also shown in Figure 5B.

The predicted pH dependence of the fluorescence emission of the adduct (for concentrated solutions), eq 5, fits well the experimental curve and is coincident with the difference between diluted and concentrated fluorescence titration curves (Figure 5B).

Time-Resolved Fluorescence. Figure 6 shows the fluorescence decays for compounds **L1**, **L2**, and **L3**. In general for compound **L1**, as can be seen from Figure 6, three different decay times are observed at the three studied emission wavelengths: 320, 365, and 480 nm. A collection is made at 480 nm (shifted 20 nm relative to the long-wavelength band maximum) to avoid spectral overlap of the 365 nm emission band. In general, the decay times obtained should be considered to be identical and independent of the wavelength of emission, although some scatter in the values is observed (Figure 6). In the case of **L1**, independently for the emission wavelength and pH, the decays were found to fit to double exponential laws. The data were collected at the wavelength in which the emission of each chromophore is dominant (Figure 6). This means that only three excited-state species are emitting, but these are dependent on the degree of protonation because the decay times change (decrease) with pH. For **L1**, the time dependence of the fluorescence collected at the three different wavelengths is given by

$$I_{320}(t) = a_{11} e^{-\lambda_1 t} + a_{12} e^{-\lambda_2 t} \tag{6}$$

$$I_{365}(t) = a_{21} e^{-\lambda_1 t} + a_{23} e^{-\lambda_3 t} \tag{7}$$

$$I_{480}(t) = a_{31} e^{-\lambda_1 t} + a_{33} e^{-\lambda_3 t} \tag{8}$$

where λ_i is the reciprocal of the decay times, τ_i, and a_{ij} is the pre-exponential factor associated to these decay times at different wavelengths. Note once more that the emission wavelengths were chosen to have the major contribution of one of each species at that wavelength.

It can be seen that at $\lambda_{em} = 320$ nm (where Np emission is dominant) the biexponential fluorescence decays show a shorter component, with values ranging from 2.5 to 3 ns (Figure 6), resulting from the contribution of the phenanthroline emission at that wavelength (which can be compared with decay times for the **L2** chromophore in concentrated solutions in Figure 7) and a second longer decay time that is assigned to the decay of the Np chromophore. In this last case, the attribution is also made by comparison with similar polyaminic systems, such as **L3**, where an identical lifetime value is found.[6,10,11] In fact from Figure 6, it can be seen that this value ranges from ∼32 to ∼35 ns, whereas with parent systems, similar values were obtained.[6,10,11]

The fluorescence decays at the two other emission wavelengths of **L1** (365 and 480 nm) can be properly fitted with sums of two exponentials, with values of $\tau_1 \cong 3$ ns

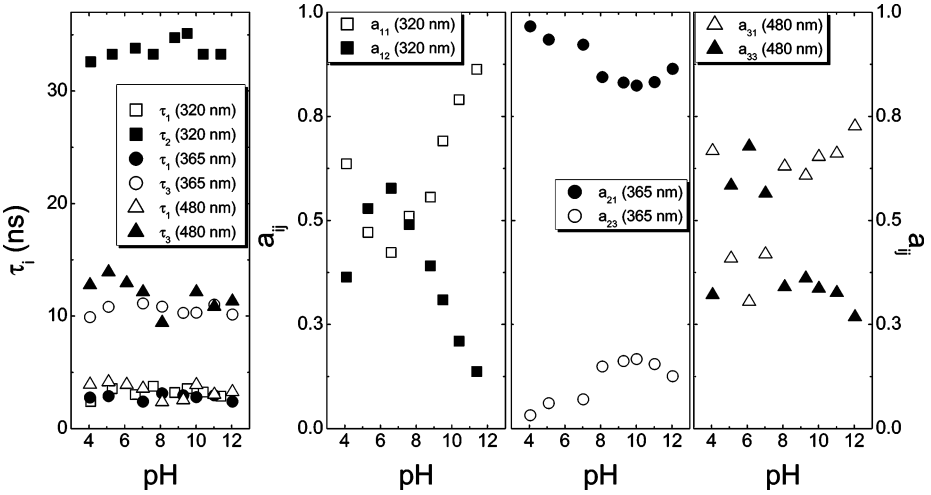

Figure 6. Dependence of fluorescence decay times, τ_i, and pre-exponential factors (a_{ij}) for **L1** at three different emission wavelengths (320, 365, and 480 nm) on pH, obtained with an independent analysis of the decays. $\lambda_{exc} = 281$ or 285 nm and $T = 20$ °C.

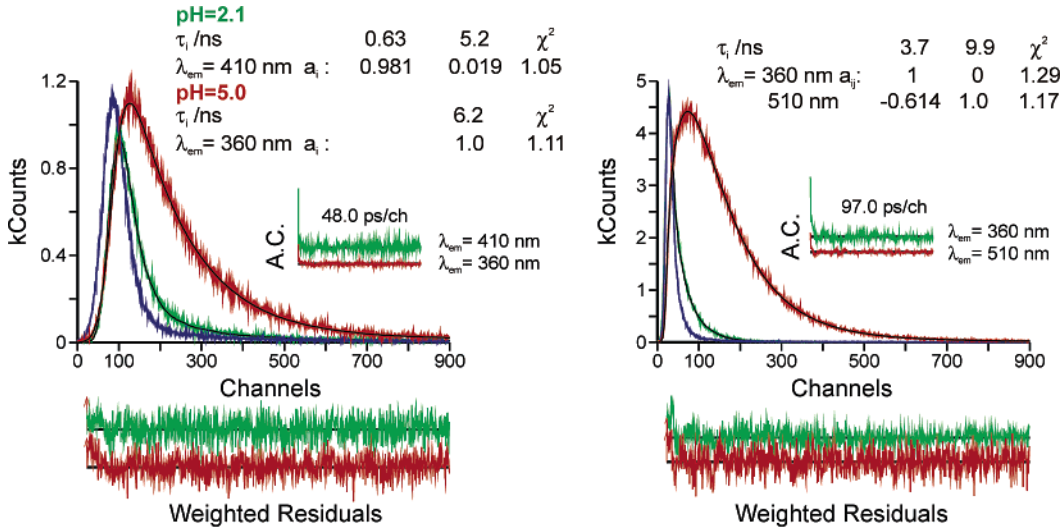

Figure 7. Fluorescence decays for compound **L2** with $[\mathbf{L2}] = 1 \times 10^{-5}$ mol dm^{-3} (left-hand panel) showing the changes in the decay profile as a function of pH and **L2** at pH 6 with $[\mathbf{L2}] = 1 \times 10^{-2}$ mol dm^{-3} (right-hand panel). Decay time values and pre-exponential values are shown as insets of the decays. For a better judgment on the quality of the fits autocorrelation (AC) functions and chi-squared (χ^2) values are shown as insets.

and $\tau_3 \cong 12$ ns. As will be shown below, the τ_1 value should be identified with the decay time of the 1,10-phenanthroline chromophore within the **L1** compound. The ≅12 ns should be attributed to the decay of the intramolecular excimer formed between the two phenanthrolines because this decay time is similar to that observed for the intermolecular excimer of 1,10-phenanthroline (Figure 7). This decay time can be clearly identified with the excimer decay as it is the predominant species at that wavelength. The lack of a rise time associated with the shorter decay time at 480 nm means that the excimer in compound **L1** is mainly (or largely) already preformed in the ground-state.

In concentrated solutions of **L2**, the decay time values in the monomer and excimer regions ($\lambda_{em} = 360$ and 510 nm) give rise to decay times of 3.7 and 9.9 ns, respectively (Figure 7). From Figure 7, it can also be seen that, contrary to what could be anticipated (because of the high concentration of **L2**), excimer formation is not only occurring through a static route but also through a dynamic process. This last process is justified by the existence of a rising component associated with the monomer decay time at 510 nm (Figure 7). The simultaneous existence of these two routes for excimer formation is supported by the positive sum of the pre-exponential factors at the excimer emission wavelength.[25]

Table 3. Time-Resolved Parameters (decay times, τ_i, and pre-exponential factors, a_i) Obtained for **L2** (1,10-phenanthroline) at Different pH Values: $\lambda_{exc} = 280$ nm, $T = 293$ K, and $[\mathbf{L2}] = 2 \times 10^{-5}$ M

pH	λ_{em} (nm)	τ_1 (ns)	τ_2 (ns)	a_1	a_2
2.1	410	0.63	5.2	0.974	0.026
3.0	410	0.42	4.5	0.981	0.019
4.2	360	–	6.2	–	1
5.0	360	–	5.8	–	1
6.3	360	–	5.8	–	1
7.0	360	–	5.8	–	1
8.0	360	–	5.6	–	1
12.1	360	–	2.9	–	1

An additional point meriting notice is the fact that, as can be observed from Figures 1 and 2, the emission of the 1,10-phenanthroline chromophore in compound **L1** occurs always from its less protonated form. This means that the specific environment generated inside the **L1** core seems to lead to

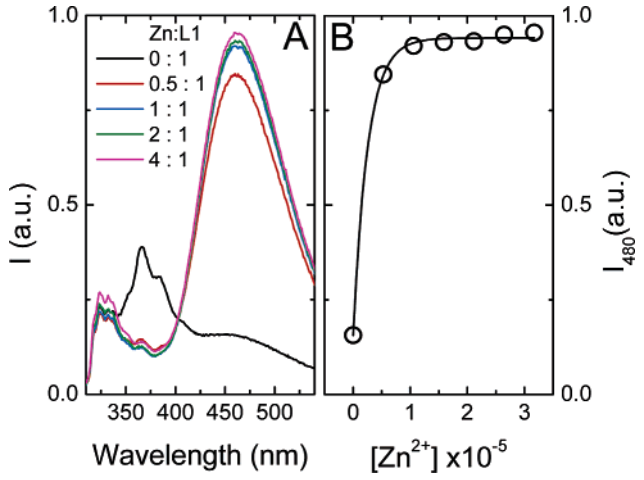

Figure 8. (A) Variation of the fluorescence emission spectra with added Zn(II) presented for molar ratios of Zn/**L1** varying from 0:1 to 4:1 of Zn(II)/**L1** and (B) presentation of the variation of the excimer intensity maximum (obtained at 460 nm) with Zn^{2+} for [**L1**] = 1×10^{-5} M. The excitation wavelength was 275 nm, and no changes in the absorption spectra were noticed with the addition of Zn(II).

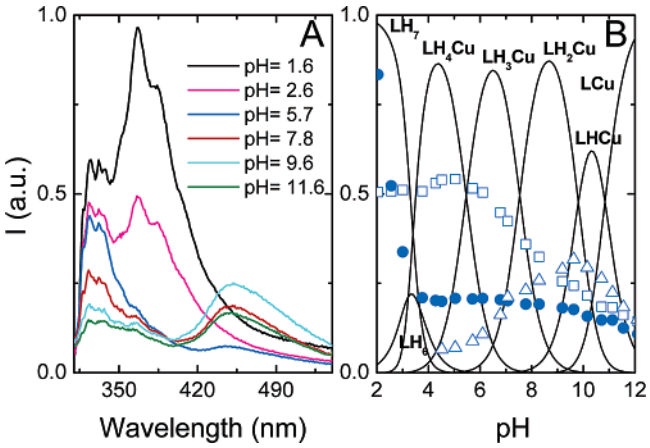

Figure 9. (A) Fluorescence emission spectra of Cu/**L1** (molar ratio 1:1) as a function of pH and (B) fluorescence emission titration curves for Cu/**L1** (1:1) obtained with λ_{exc} = 275 nm and λ_{em} = 323 (□), 366 (●), and 450 nm (△) at T = 20 °C. The dashed lines represent the molar fractions of the species obtained from potentiometric titrations.

a situation where the nonprotonated phenanthroline is the emitting species. In fact, the variation with the pH (Table 3) of the decay times obtained for **L2** diluted solutions (where no intermolecular excimer is present) displays a double-exponential behavior at acidic pH values, resulting from the contributions of the protonated phenanthroline, with a lifetime of ∼500 ps, and the unprotonated form, with a lifetime ∼6 ns. The shorter component progressively disappears with the increase in pH, resulting in single-exponential behavior above pH 4.2 (Figure 7 and Table 3). Simultaneously, the steady-state emission spectra for diluted solutions of **L2** (phenanthroline) show that at acidic pH values the emission band is settled with a maximum at 410 nm, whereas at neutral and alkaline pH values, this band disappears resulting in a structured emissive band at a shorter (360 nm) wavelength maximum (Figure 4B), which is identical to the band observed for **L1**.

Interaction with Metal Cations. Coordination with Zn(II). The interaction between **L1** and Zn(II) was performed for different Zn(II) to **L1** ratios (Zn/**L1**) to establish the effective stoichiometric ratio. In Figure 8, it can be seen that the maximum increase in the excimer emission is achieved for a Zn/**L1** ratio of 1:1, although there is still a slight increase upon addition of more equivalents of Zn(II).

From the titration curve (see Supporting Information), it can be seen that in the presence of Zn^{2+} it is only after pH > 3.2 that the 460 nm band, previously attributed to an excimer, begins to be visible, whereas in the case of **L1** alone this band was visible only for pH values higher than 4 (Figure 1). Moreover, there is a large enhancement of the excimer band intensity in the case of the coordination complex Zn/**L1** (1:1) (LH_4Zn and LH_3Zn forms) when compared to that of **L1** alone at identical pH values. This suggests that the interaction between the two phenanthroline units is more efficient upon Zn(II) complexation. Upon coordination with Zn(II), an increase in the fluorescence emission is observed. Moreover it can be observed that LH_4Zn is the most emissive species (see Supporting Information). This happens because, with this species, all the nitrogens of **L1** are either bonded to the Zn(II) or protonated, avoiding any suppression of the emission by electron-transfer quenching.[14,26] The fact that the maxima of the three bands relative to the three chromophores do not change when coordinated with Zn(II) is also of relevance.

Interaction with Metal Cations. Coordination with Cu(II). In the case of the Cu/**L1** coordination complex, and in comparison with Zn/**L1** and **L1**, there is a general quenching of the overall emission spectra, in particular of the excimer emission. This is usually associated with the well-known chelation-enhanced quenching effect (CHEQ) phenomena, which occurs with metal ions, such as Cu(II), that have uncompleted d orbitals.[11] In the present case, this effect only takes place for pH > 4 where the LH_3Cu species is predominant in solution (Figure 9). It is also visible that the wavelength maximum of the excimer band shifts toward the blue when **L1** is coordinated with Cu(II). In fact, the emission maximum of the excimer in this case is settled at ∼450 nm, which is different from the longest emission wavelength band found for **L1** and for the Zn/**L1** coordination complex (observed with a maximum at 460 nm). This wavelength shift of ca. 10 nm could reflect the different geometric arrangements upon coordination of both metals. It is interesting to note here that the excimer emission becomes important only for pH values above 6 (LH_2Cu and LHCu species), and this could reflect rearrangements in the complex upon deprotonation.

Conclusion

We have performed a comprehensive study on the photophysical properties of a new ligand possessing two phenanthroline chromophores as chelating units. The emission spectra of the compound, displaying three emissive bands, were found to be pH dependent. Two of the bands are attributed to the emission of the phenanthroline and naphthalene chromophores, whereas the additional long-wavelength emissive band (only present for pH values above 4)

was attributed to a new excimer species resulting from the interaction between one excited phenanthroline and one phenanthroline in the ground state. In the case of the coordination with metal cations Zn(II) and Cu(II), a chelation-enhanced fluorescence effect with the zinc and a chelation-enhanced quenching effect with Cu(II) were observed. Moreover, the excimer emission in the case of Cu(II) coordination was found to be blue-shifted relative to that of the ligand alone or coordinated with Zn(II). This could potentially establish this ligand as a sensor for Cu(II).

Acknowledgment. This work was supported in part by FCT Project 47357/02 (Portugal), the European Community's Human Potential Program (under contract HPRN-CT-2000-00029, Molecular Level Devices and Machines) and the Generalitat Valenciana GV04B-225, Grupos S03/196, and DGICYT Project BQU2003-09215-CO3-01 (Spain). R.A. wants to thank MCYT for a predoctoral grant. J.P. acknowledges FCT for a Ph.D. grant (SFRH/BD/18876/2004).

Supporting Information Available: Additional information including the distribution diagram as a function of pH for the system Cu^{2+}−**L1** (2:1 and 1:1 ratios), the absorption spectra of compounds **L1**, **L2**, and **L3** at pH 2.0 and 6.0, the decomposed fluorescence emission spectra of concentrated (1.7×10^{-2} M) 1,10-phenanthroline, the titration curve (B) for **L1** in the presence of Zn^{2+} (1:1), and the complete kinetic scheme translating the adduct formation in the case of 1,10-phenanthroline in concentrated solutions together with its fluorescence emission spectra as a function of pH. This material is available free of charge via the Internet at http://pubs.acs.org.

IC050733Q